NMR nowadays!

NMR Overview:

The technique has developed rapidly during its brief history. Advances in instrumentation, especially magnet technology has allowed many different applications.

The applications fall into three fairly different groups:

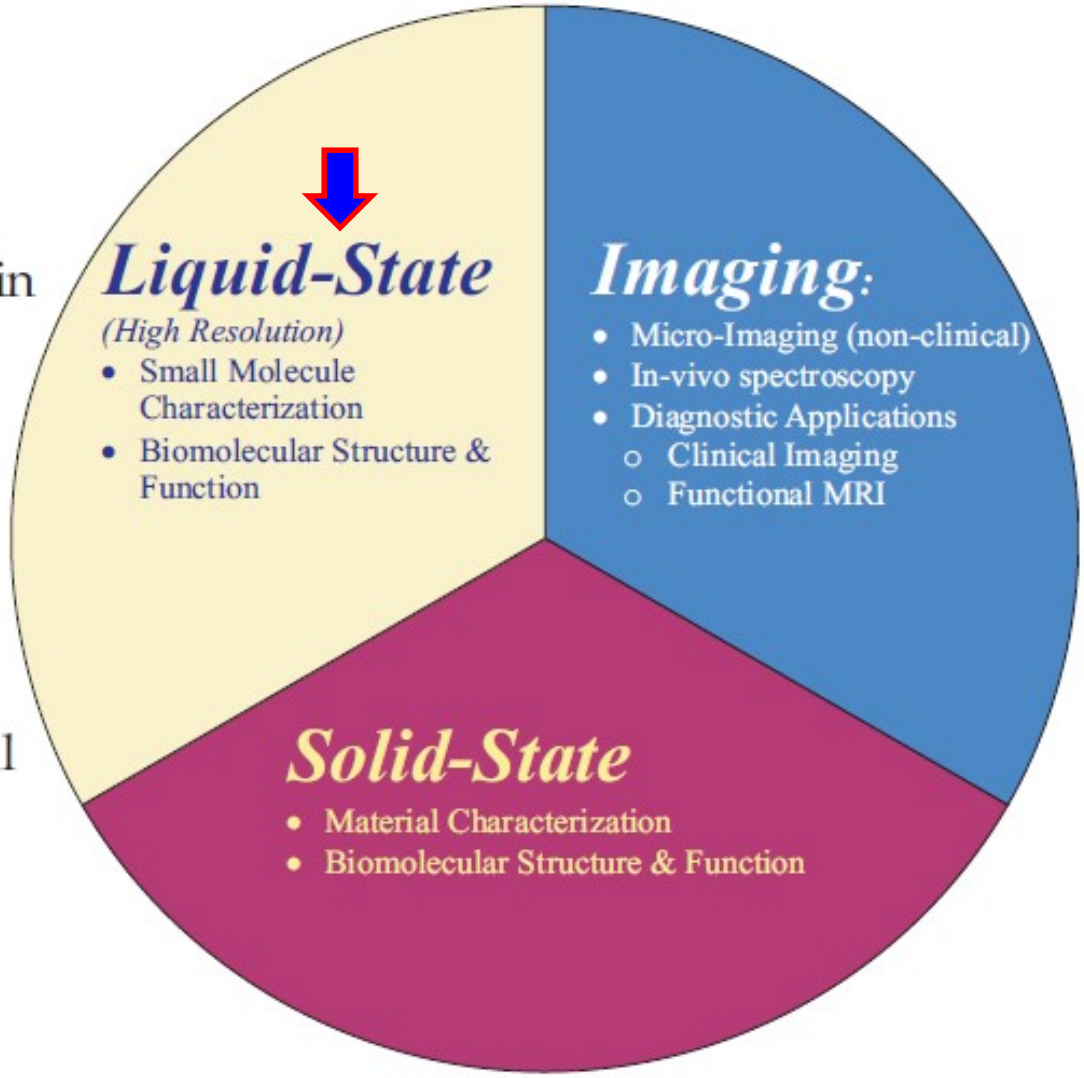

NMR timescale

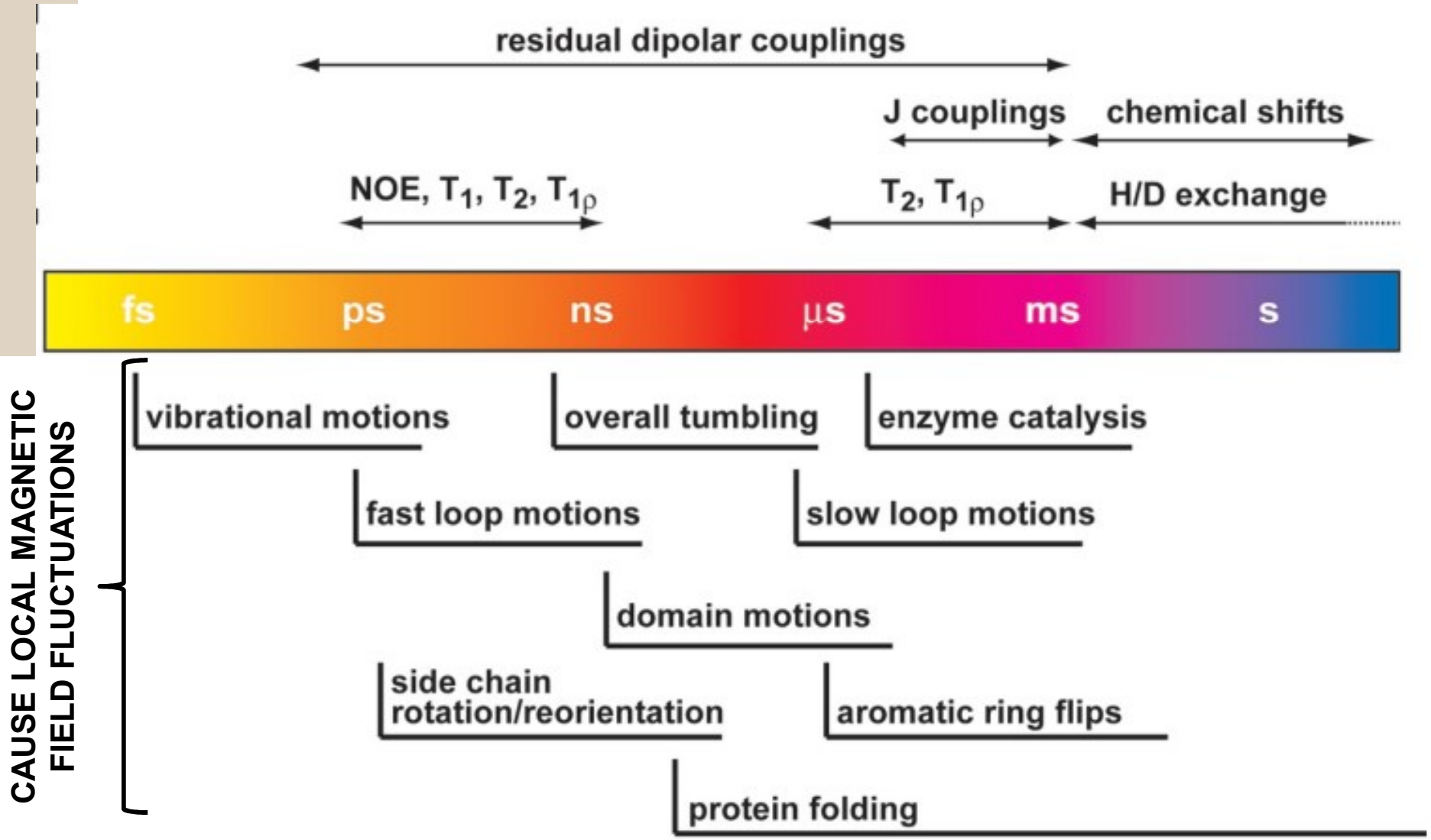

Structural constraints (NOE vs RDC)

- Traditional NOE-based 3D structure determination methods suffer from the lack of long-range structural restraints (limitation is up to 5-6 Å).
- In this context, "long-range" means parts of the compounds not close in space and thus, not measurable by NOE methodology.
- For assessing 3D structures where there is limited contact between the internal parts, it is often difficult to properly orient the structural components with respect to one another (using only NOE-based restraints).
- Residual dipolar couplings (RDCs) afford a route to effective long range orientational (not translational) restraints.
- RDCs allow orientation of bond vectors with respect to a reference axis (typically *z-axis,* B_0 direction in the laboratory frame).
- Therefore, these restraints effectively constrain bond vectors relative to one another, which amounts to long-range conformational/orientational restraints.

Review papers for further studies

- Prestegard, A-Hashimi & Tolman, *Quart. Reviews Biophys.* ***33, 371-424*** (2000)***.***
- Bax, Kontaxis & Tjandra, *Methods in Enzymology,* **339, 127-174** (2001).
- Prestegard, Bougault & Kishore, *Chemical Reviews,* ***104, 3519-3540*** (2004).
- Lipsitz & Tjandra, *Ann. Rev. Biophys. Biomol. Struct.,* ***33, 387-413*** (2004).
- Fushman et al., *Prog. NMR Spect.* ***44, 189-214*** (2004).
- Hu & Wang, Ann Rpts NMR Spect, **58,231-303** (2006).
- Bailor et al., Nature Protocols, **2, 1536-1546** (2007).
- Prestegard. *Nat Struct Biol.,* 5, 517-22 (1998).

The Dipole-Dipole Interactions

- Through space interaction between dipoles
- Angular dependence (θ and ϕ)
- Distance dependence (r)
- Dipolar splittings average in solution (not observed), but are present in solid state
  - are complicated, and dominate solid state spectra

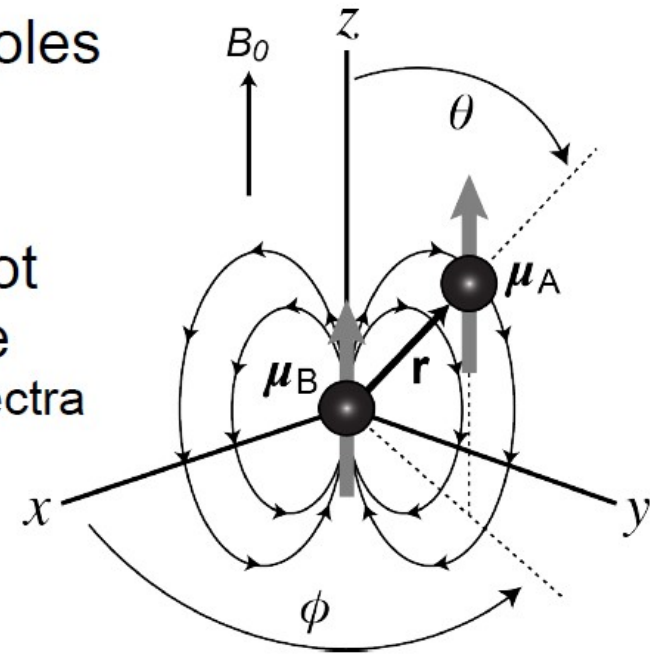

- Important parts: $1/r^3$ dependence, angular dependence

The Dipole-Dipole Interactions

- Consider signal splitting due to dipolar coupling (solid state)

$$\hat{\boldsymbol{H}}_{\mathrm{D}} = \frac{\mu_0 \gamma_I \gamma_S h^2}{(16\pi^3 r^3)}(-\hat{\boldsymbol{I}}_z \hat{\boldsymbol{S}}_z (3\cos^2\theta - 1))$$

- In solid state, result is doublet with $1/r^3$ and $(3\cos^2\theta - 1)$ dependencies
  - in solid state (powder), all possible values of θ are present, so result is a superposition of all possible signals with all possible couplings
  - splittings are large (~60 kHz for ^{13}C-^{1}H, ~250 kHz for ^{1}H-^{1}H)
  - splittings are angle dependent (-60 kHz to +30 kHz for ^{13}C-^{1}H)
- In solution, θ is averaged, so no splitting is observed

Dipolar Splitting in Solid-State (Powder) Spectra

- In the solid state, chemical shift anisotropy leads to broad signals due to presence of signals from all possible molecular orientations
- Dipolar splittings result in very broad doublets

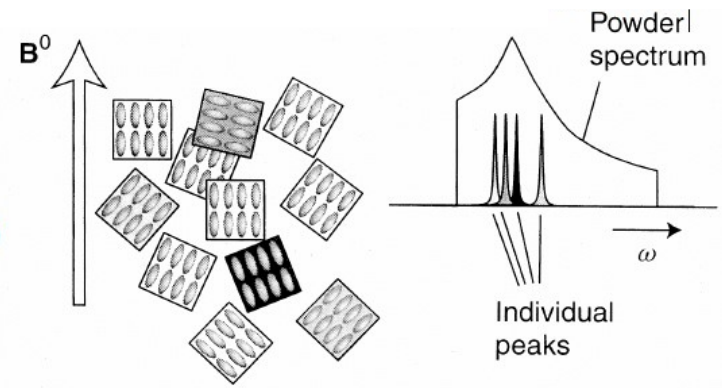

- Consider various values of θ (and all possible values of ϕ)
  - values of θ and ϕ define a sphere (for some fixed r, i.e. C-H bond))
  - *largest splittings* (most positive) *are when* $\theta = 0$ ([$3\cos^2\theta - 1$] is largest when $\theta = 0°$): this is a single point on the sphere, so, not highly populated (low intensity, but largest splitting, ~60 kHz for C-H)
  - *smallest splittings* (most negative) *are when* $\theta = 90°$ ([$3\cos^2\theta - 1$] is smallest when $\theta = 90°$): this is around the equator of the sphere, so, highly populated (high intensity, but smallest (most negative) splitting)
  - when $\theta = 54.7°$, $3\cos^2\theta - 1 = 0$, so no splittings at that value of θ

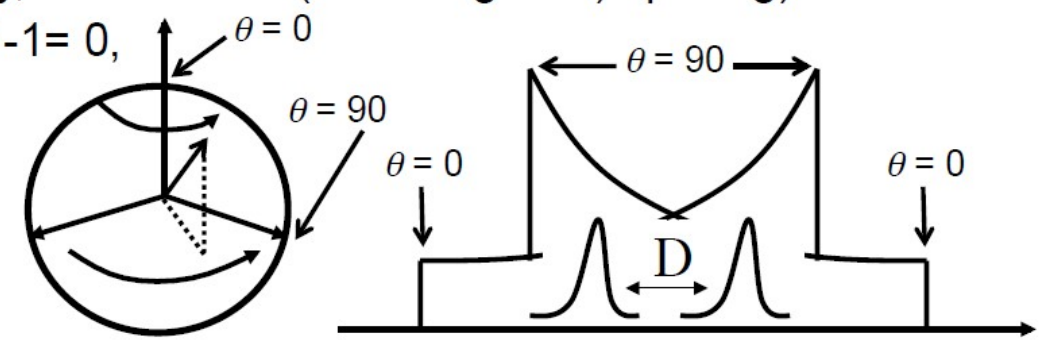

Orientations of RDC-generated vectors

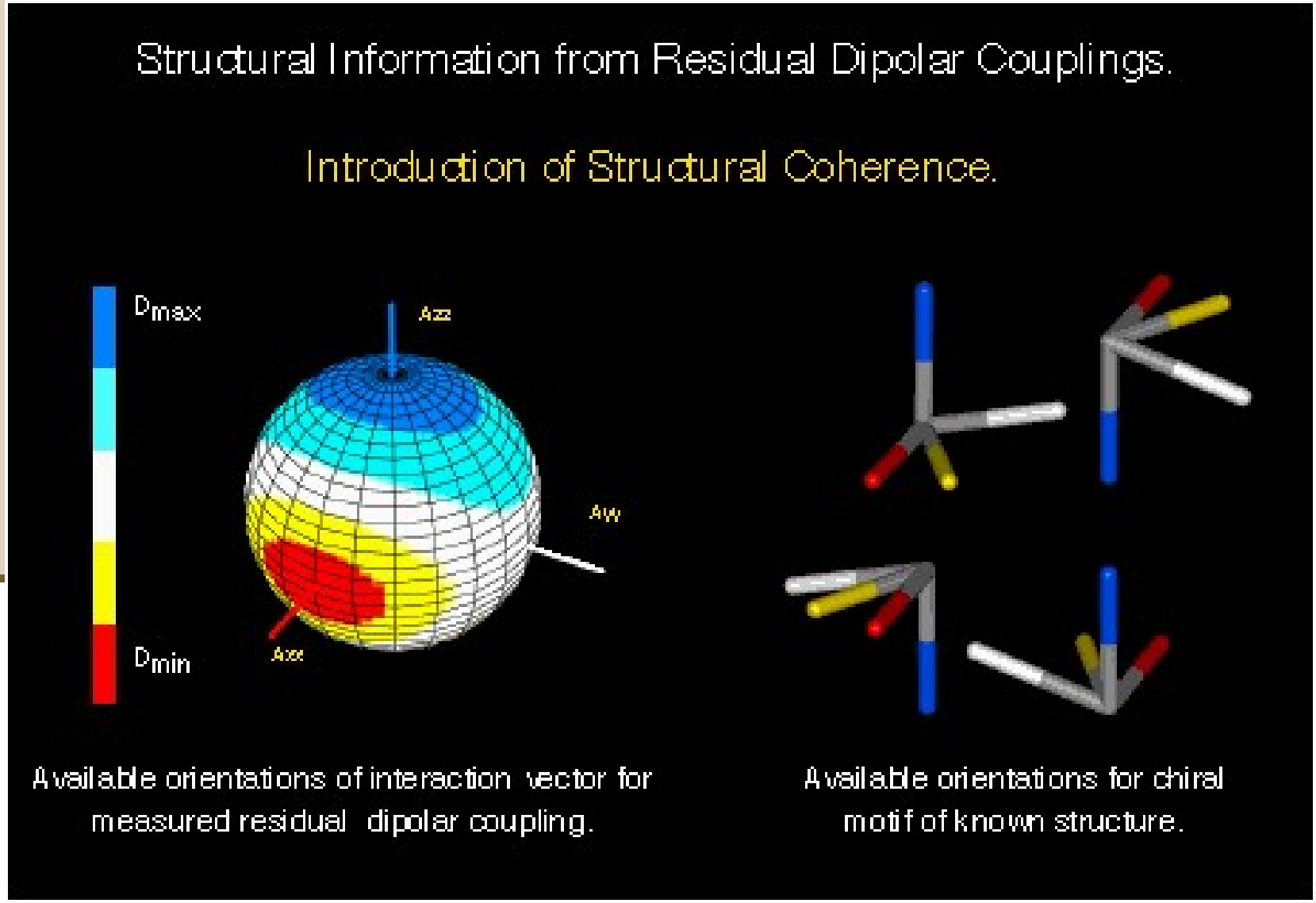

Dipolar Couplings Add to the Multiplet Splittings

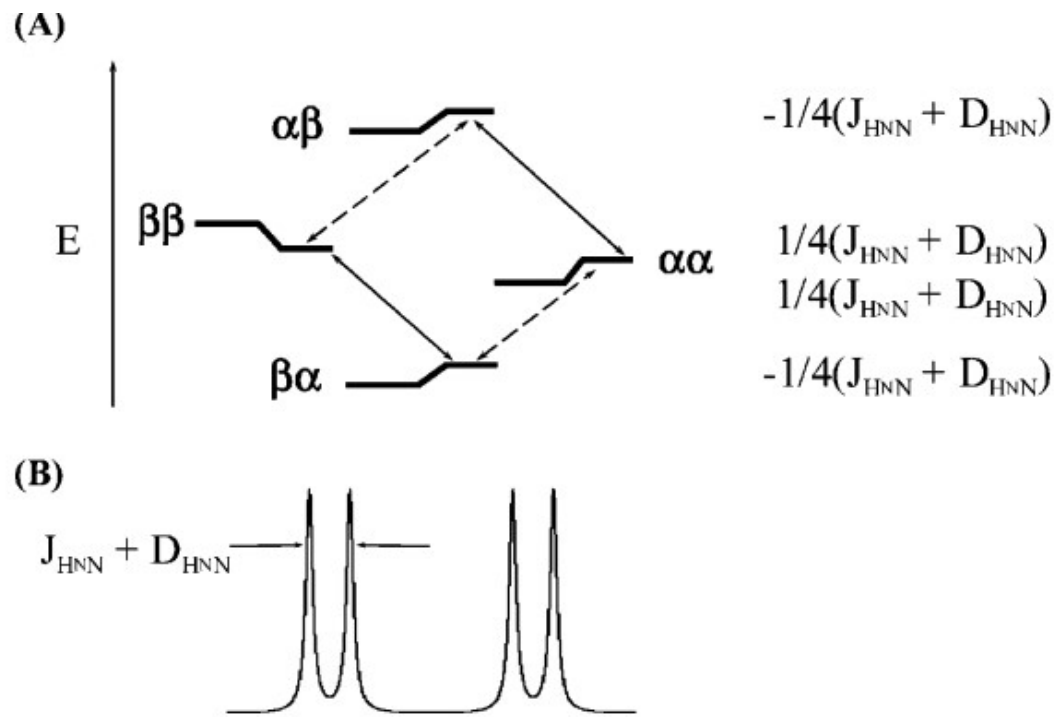

Figure 1. (A) Energy level diagram for a $^{1}H-^{15}N$ spin system. The dashed arrows are ^{15}N transitions, and the solid arrows are ^{1}H transitions. The effects of scalar and dipolar couplings, assuming a negative $J + D$ value, are denoted to the right of the diagram. (B) The expected ^{15}N and ^{1}H doublets are shown at the bottom.

Measurements of Residual Dipolar Coupling

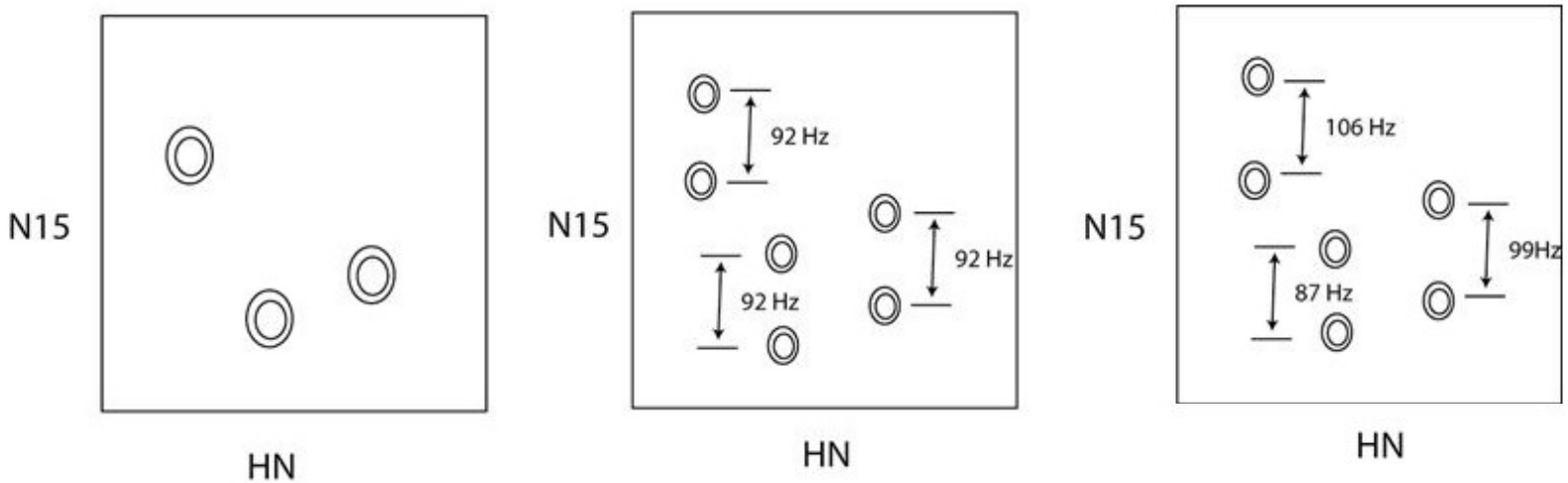

--regular HSQC
--decoupled in both dimensions
--^{15}N-^{1}H splittings not observed

--HSQC without decoupling in ^{15}N dimension
-- ***isotropic solution***
--^{15}N-^{1}H splittings observed, equal to ^{15}N-^{1}H one-bond scalar coupling (~92-95 Hz)

--HSQC without decoupling in ^{15}N dimension
--***partly oriented***
--^{15}N-1H splittings observed, equal to ^{15}N-^{1}H one-bond scalar coupling plus RDC!
Some RDC -, some +

Residual Dipolar Coupling: dipole-dipole vectors

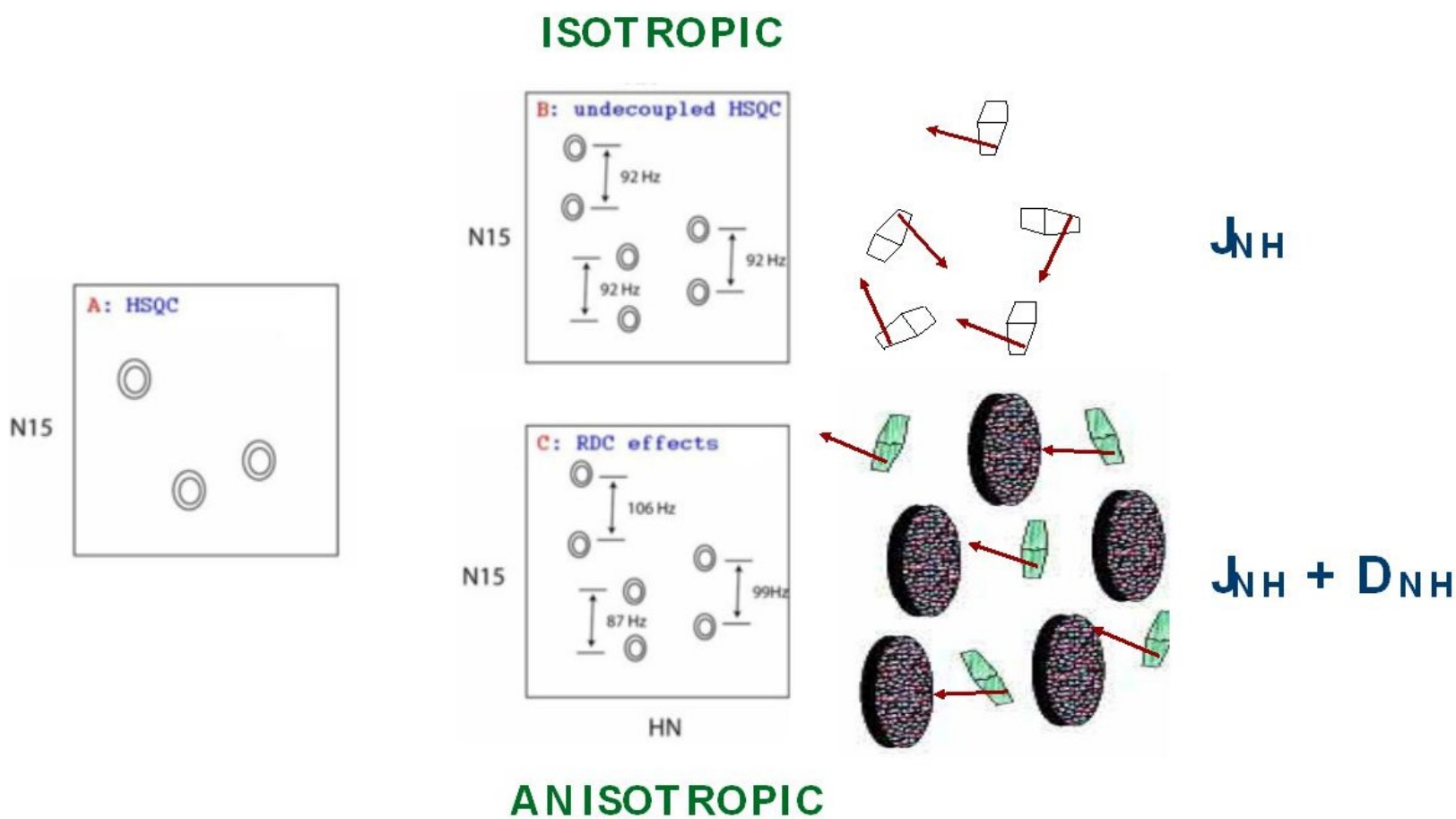

⇒ Difference gives RDC D_{NH}

The role of decoupling in HSQC spectra

^{1}H-^{13}C HSQC spectra of benzene

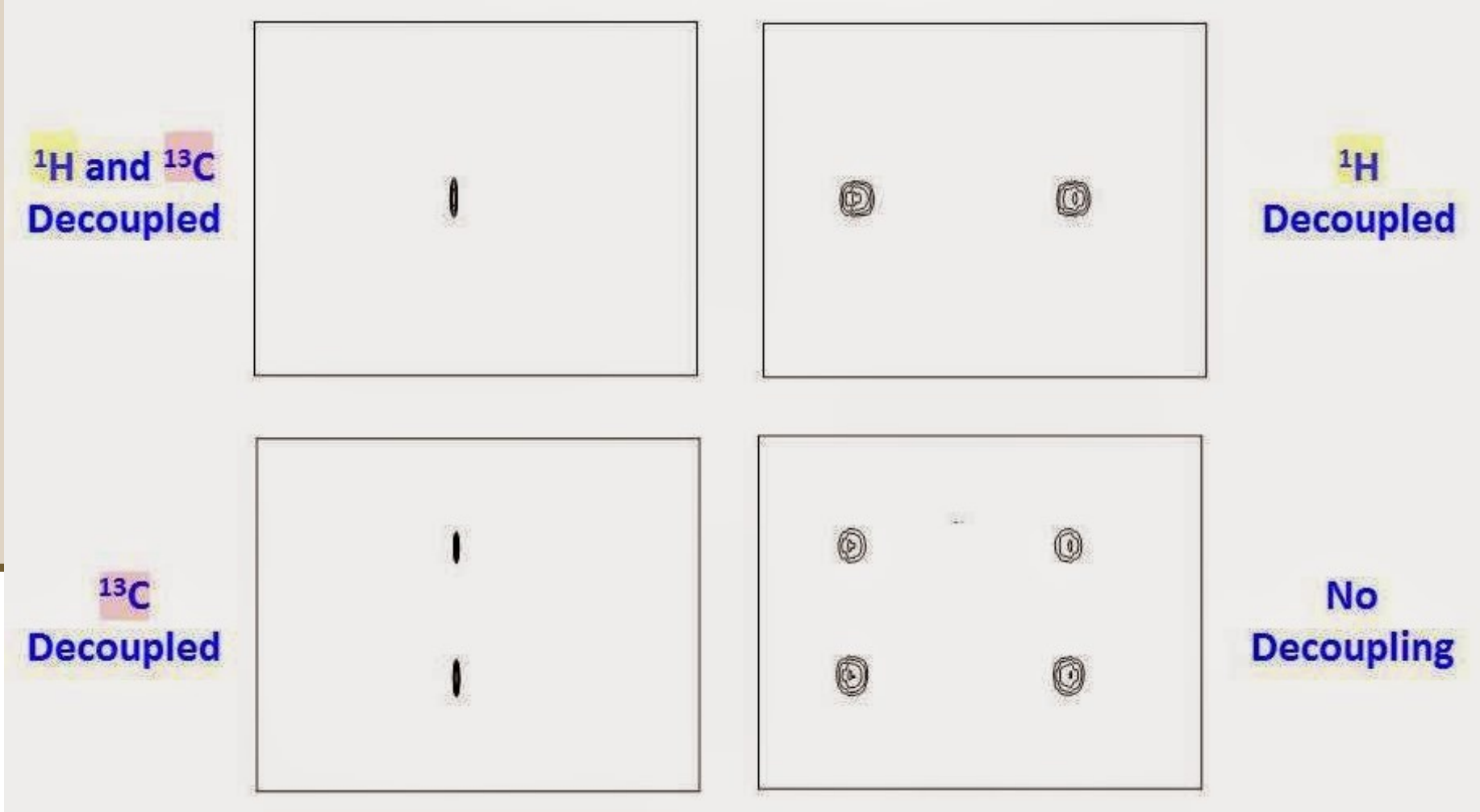

Decoupling elements in gHSQC pulse sequence

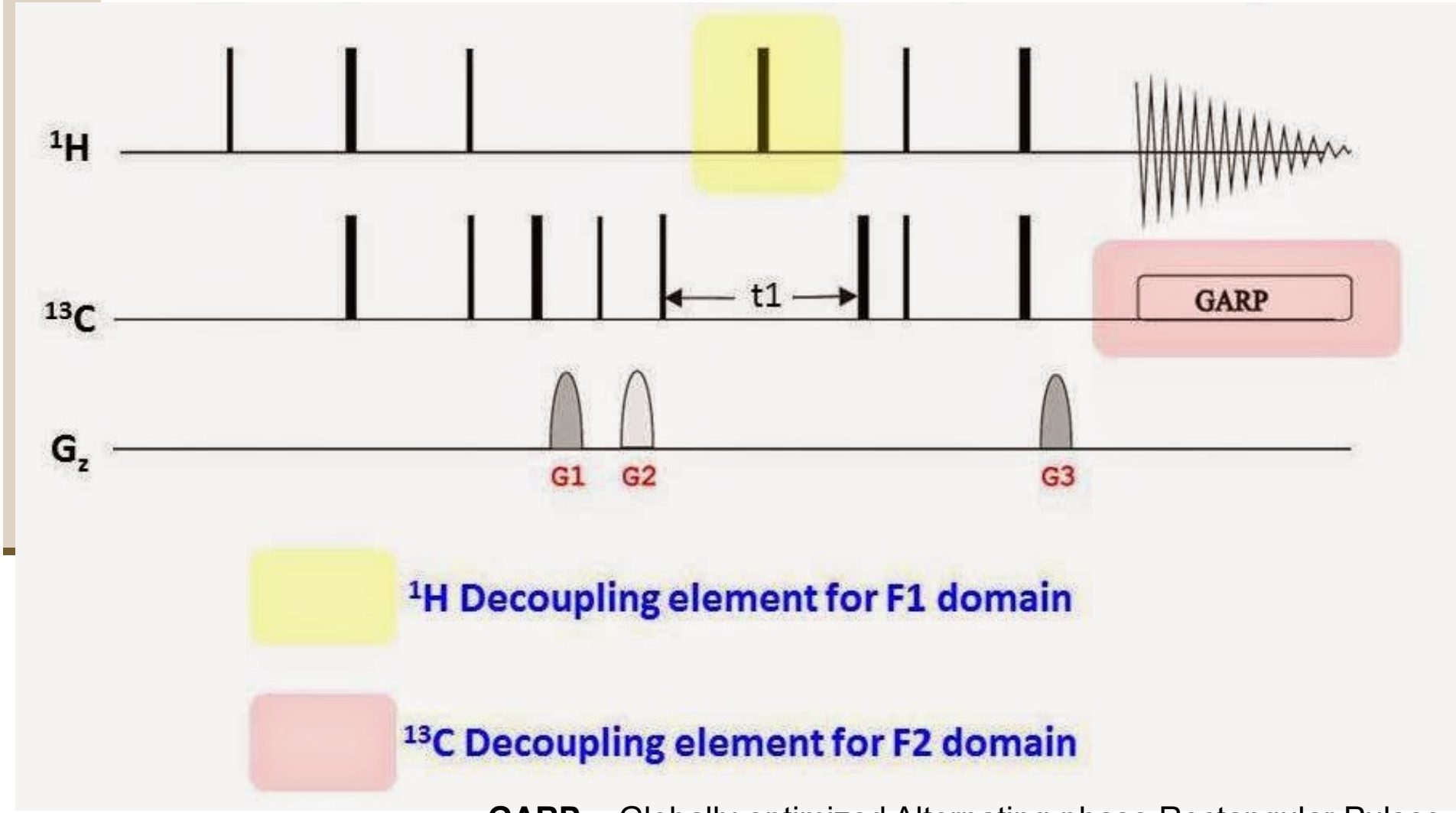

GARP = Globally-optimized Alternating-phase Rectangular Pulses

Isotropic condition

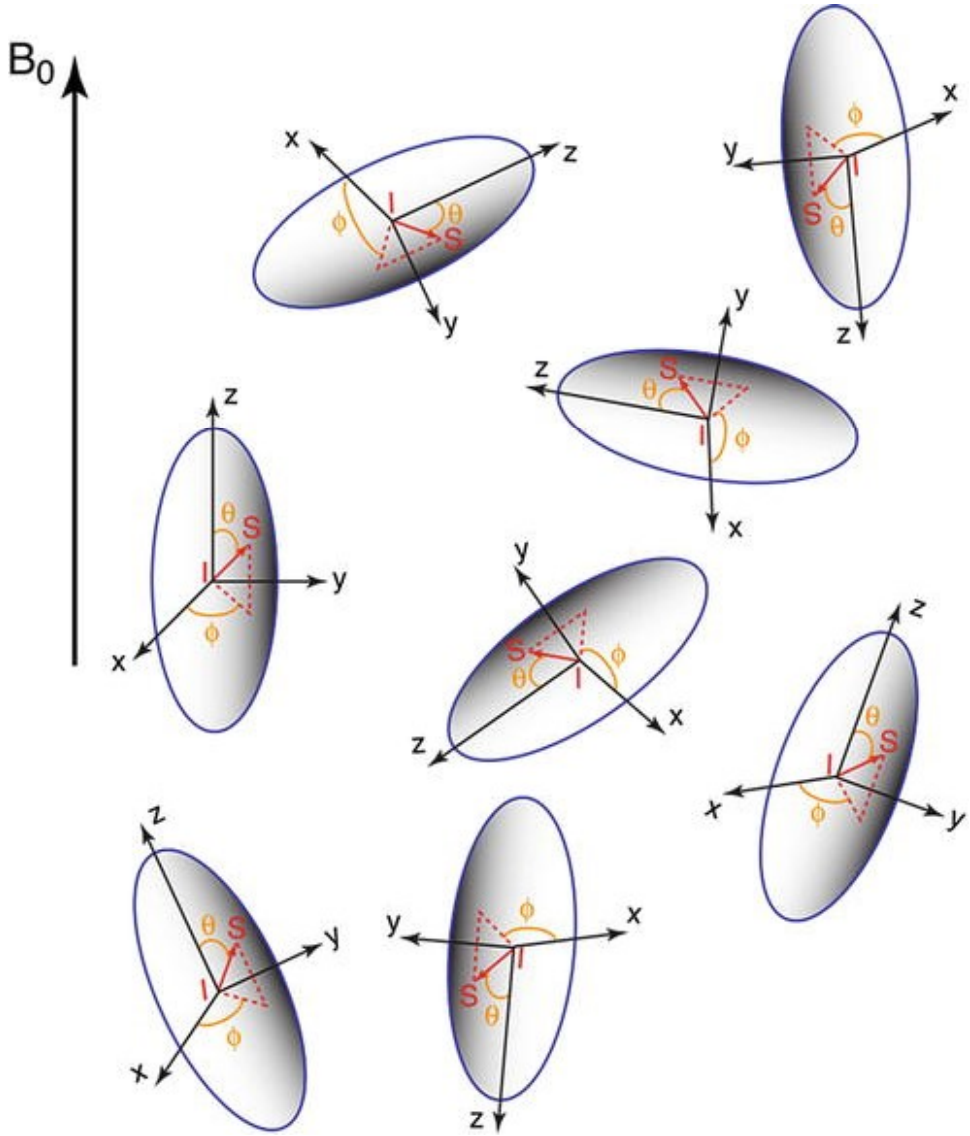

Isotropic vs Anisotropic (deuterium signal)

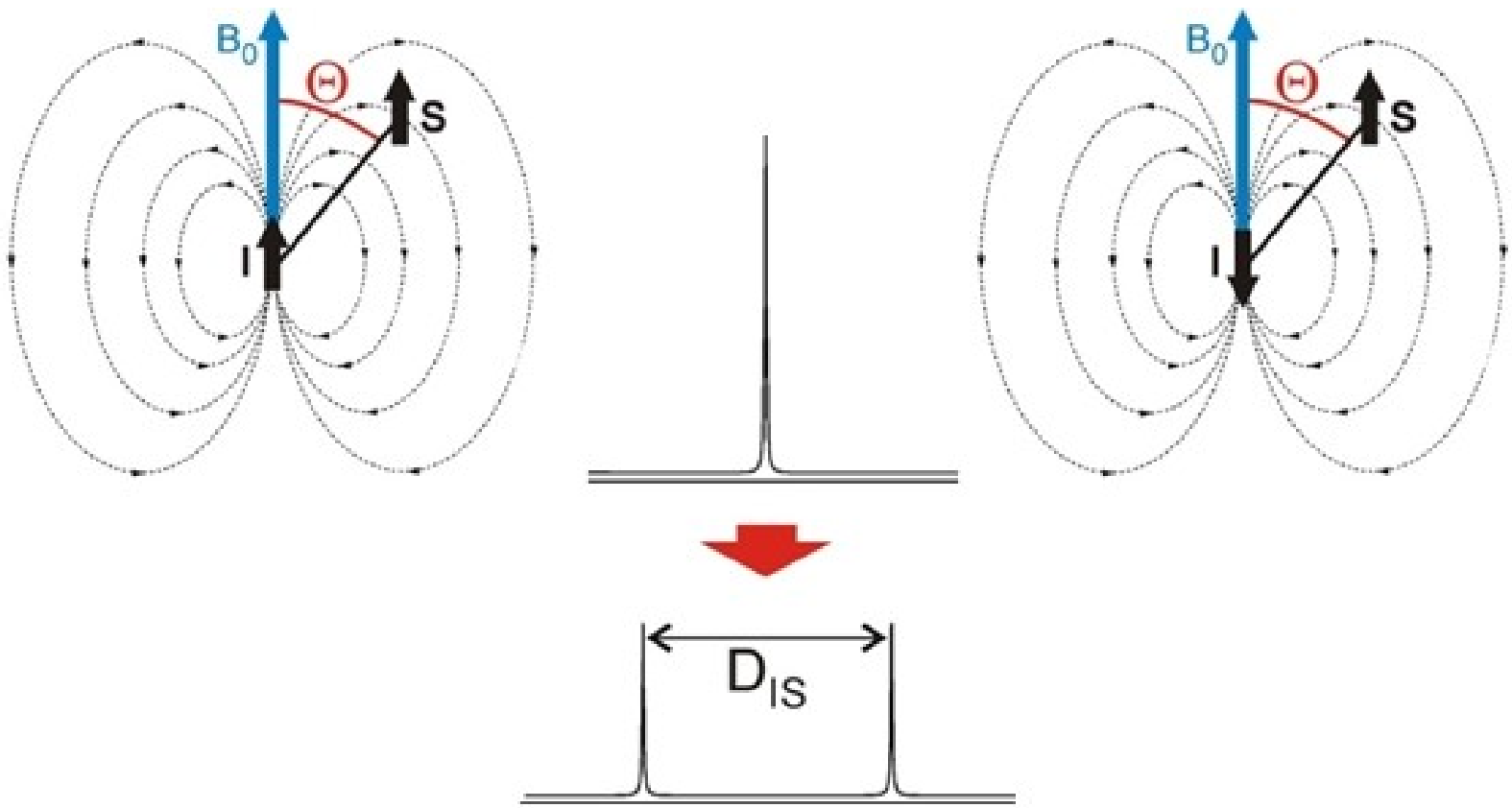

$$D \sim (3 \cos^2 \Theta - 1)\, r^{-3}$$

Isotropic vs Anisotropic

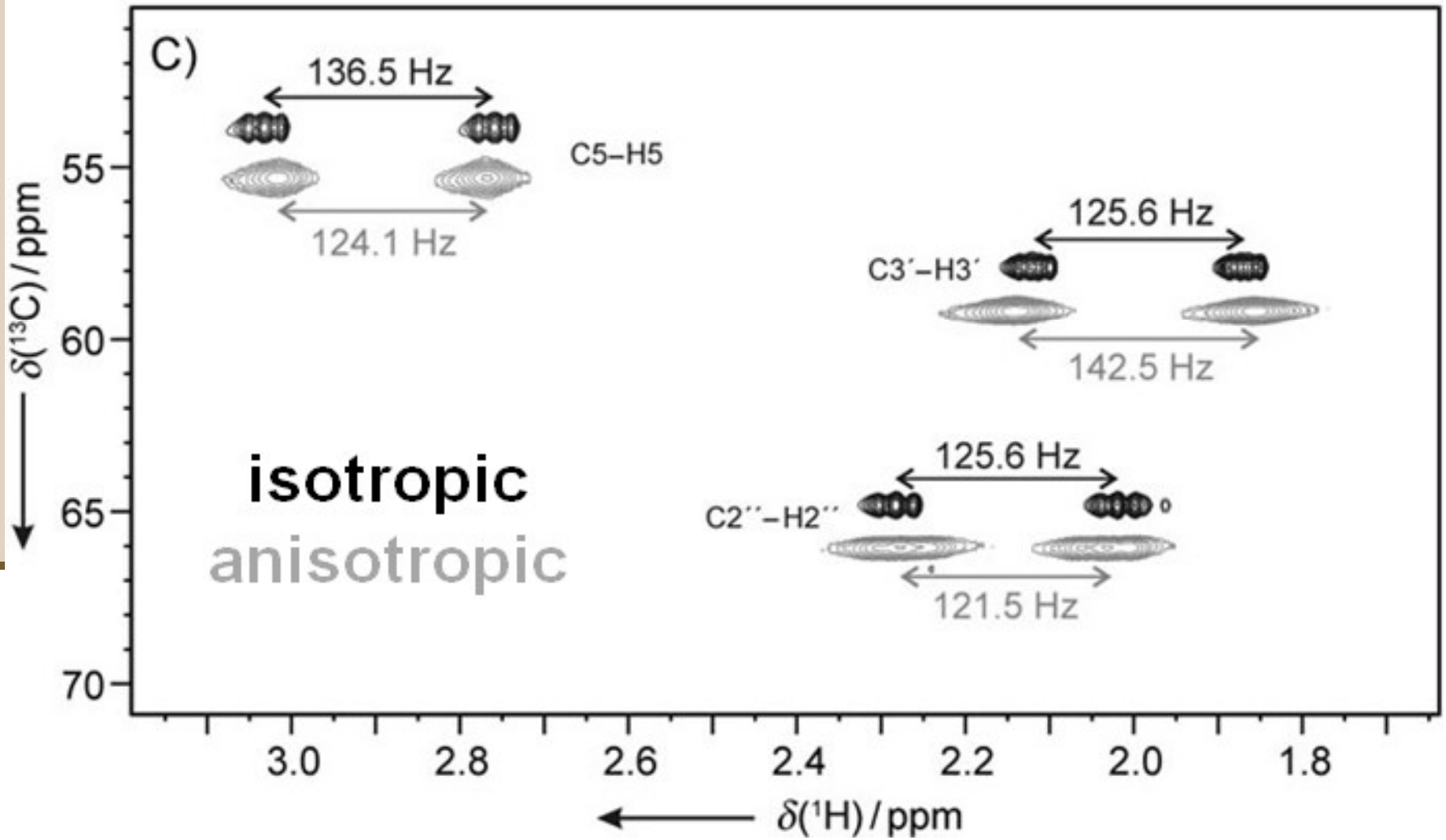

Inducing alignment for oriented NMR

- other mechanisms (electrostatics) can also contribute to alignment
- dipolar coupling observed as change in scalar (*J*) coupling in the isotropic versus partially aligned state

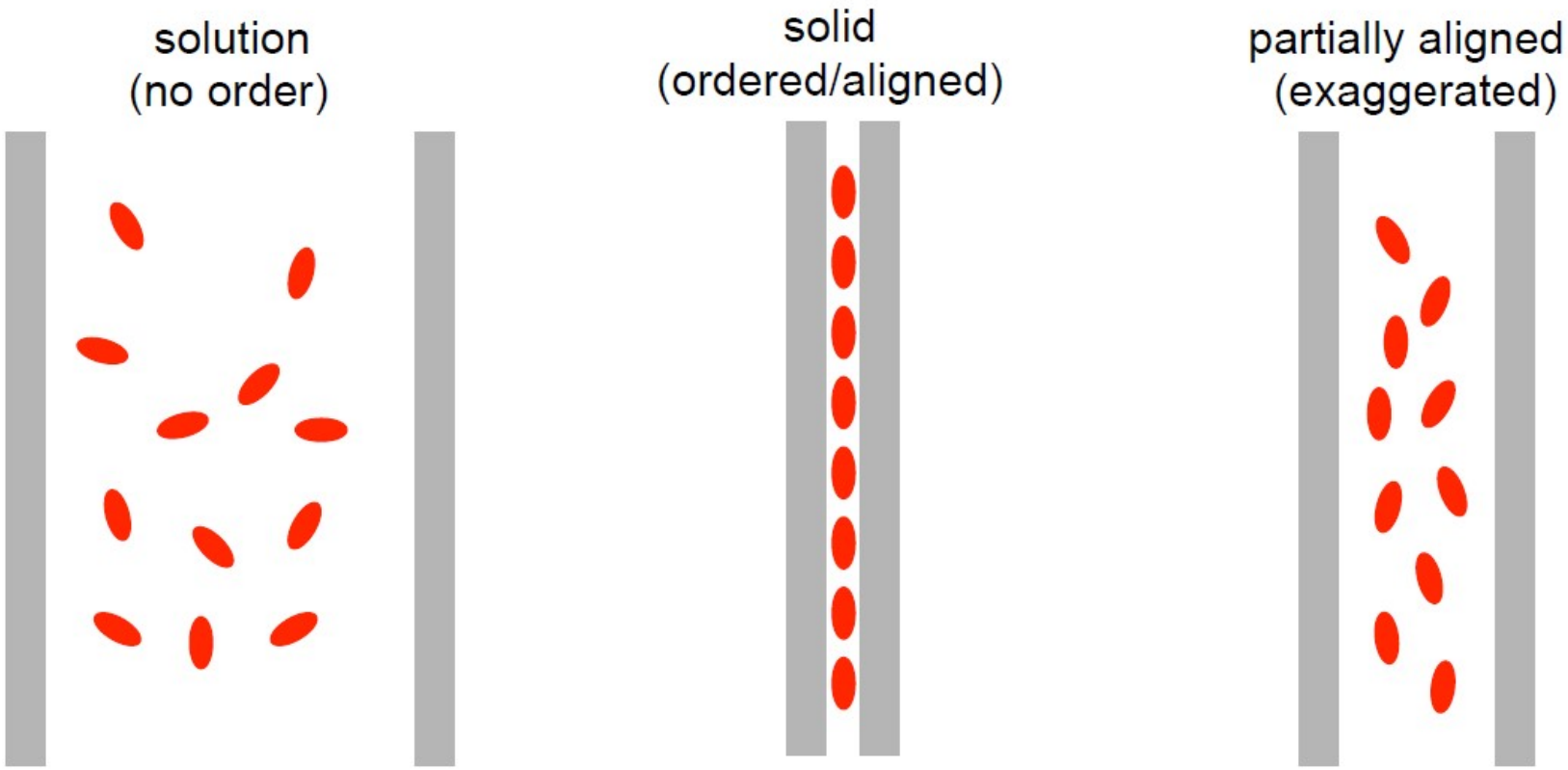

Alignment Media

Table 1. Alignment Media Commonly Used to Measure Residual Dipolar Couplings

medium	molecular species	charge	temp range (°C)	features and limitations	ref
ester-linked phospholipid bicelles	DMPC/DHPC	neutral	27−45	+ easy preparation − expensive, susceptible to hydrolysis	2 183
ether-linked phospholipid bicelles	DIODPC/CHAPSO DIODPC/DIOHPC	neutral	10−55	low pH	184 185
phospholipid bicelles doped with charged lipids	DMPC/DHPC/ CTAB/SDS	CTAB, positive SDS, negative	27−40		69
poly(ethylene) glycol ether bilayers	C_nE_m/*n*-alcohol	neutral	0−60	+ easy preparation, inexpensive + highly compatible with biomolecules − kinetics of alignment esp. with dissolved biomolecules unknown	186
poly(ethylene) glycol ether bilayers doped with charged lipids	C_nE_m/*n*-alcohol/CTAB/SDS	positive, negative	0−60		109
bacteriophage	rod-shaped viruses	negative	5−60	+ easy preparation, sample recovery − only suitable for negatively charged biomolecules	43, 44 187, 188
purple membranes	cooperative anisotropic membranes	charged	<70		189, 190
stretched or strained polyacrylamide gels	polyacrylamide gels	neutral	5−45	+ easy sample recovery + can accommodate larger MW (esp. membrane) proteins − difficult to align homogeneously − strong steric interactions cause broad lines	47 48 89 191
charged polyacrylamide gels	acrylamide/acrylate	charged	5−45	+ decreased line broadening − delicate and easily ruptured	50 51
immobilized media	gel- or polymer-stabilized purple membranes or phage	neutral		+ fixed director orientation	48, 192, 193
lanthanide ions/ Ln-binding tags	align by anisotropy of susceptibility			+ no compatibility problems − very small degree of alignment	54 56, 57
Helfrich phases	CPyBr/*n*-hexanol/NaBr	neutral	0−70	+ stable, wide temperature range − very sensitive to salt, buffer, pH	194 195

Inducing Order Using Liquid Crystalline Media

- Partial alignment is induced by adding protein to any of a number of types of media that promote alignment
  - liquid crystalline media, such as bicelles formed by lipids (DHPC/DMPC) or filamentous bacteriophage are some of the first and still commonly used

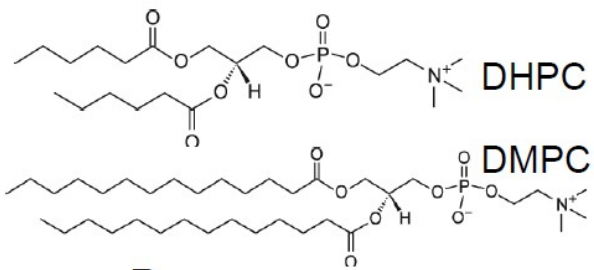

- these large have a large net induced magnetic moment in a magnetic field that causes them to align in one direction in a magnetic field
- mechanical interactions of the proteins with these particles promote the small net alignment of the proteins

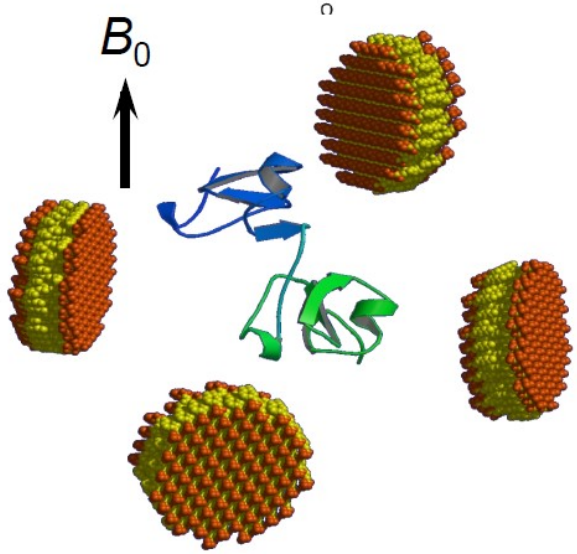

filamentous bacteriophage (Pf1)

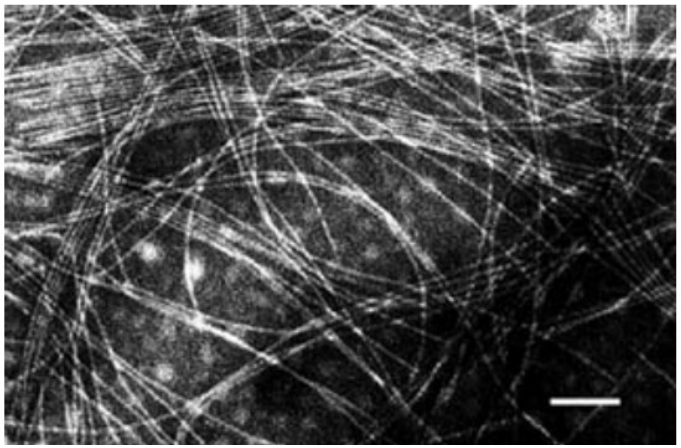

DHPC: 1,2-Diheptanoyl-sn-Glycero-3-Phosphocholine
DMPC: 1,2-Dimyristoyl-sn-Glycero-3-Phosphocholine

Measuring Dipolar Couplings - Coupled HSQC

- Are many ways to measure the residual dipolar couplings
  - simplest is just to record HSQC spectra without ^{1}H decoupling during ^{15}N evolution, under both isotropic and aligned conditions
  - difference in measured splitting is dipolar contribution

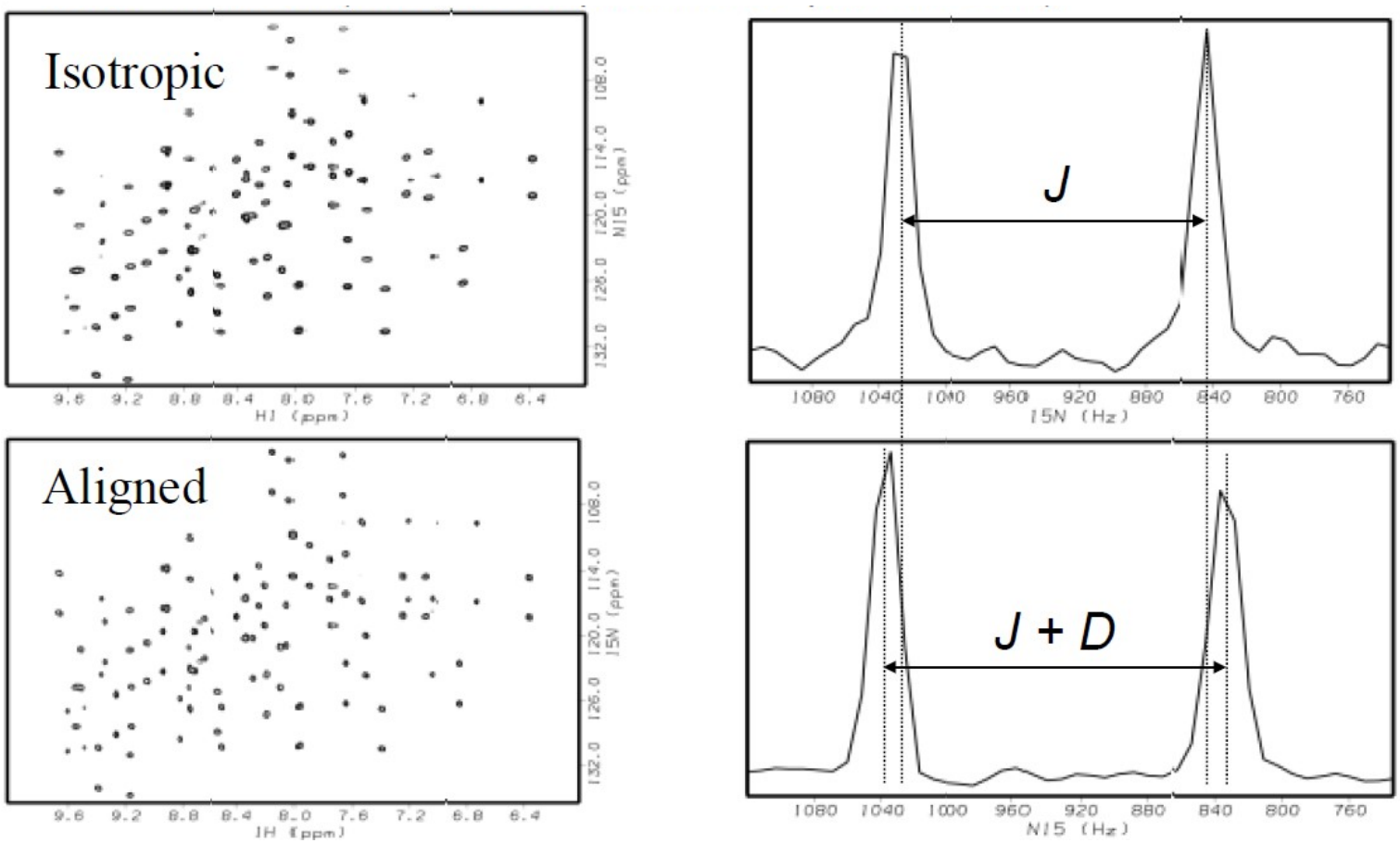

Measuring Dipolar Couplings - Coupled ^{15}N HSQC

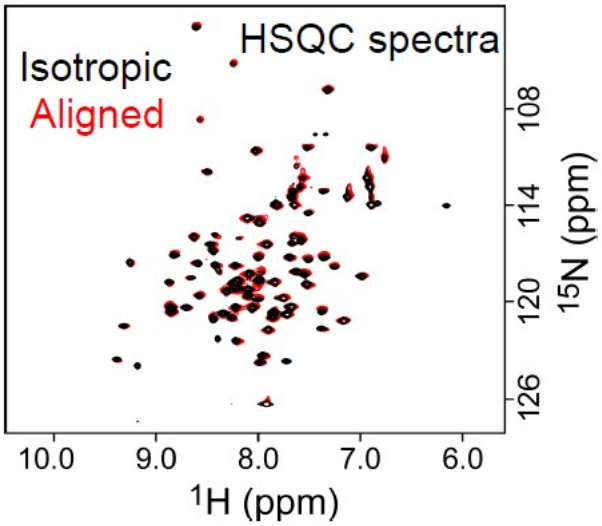

- Important to remember:
  - cannot trust measurements if alignment medium changes the protein structure (chemical shifts for each signal in HSQC spectrum for isotropic state must be identical to those in aligned state)
  - ^{1}H-^{15}N scalar coupling constants are *negative* (^{1}H-^{15}N dipolar couplings are both positive and negative)

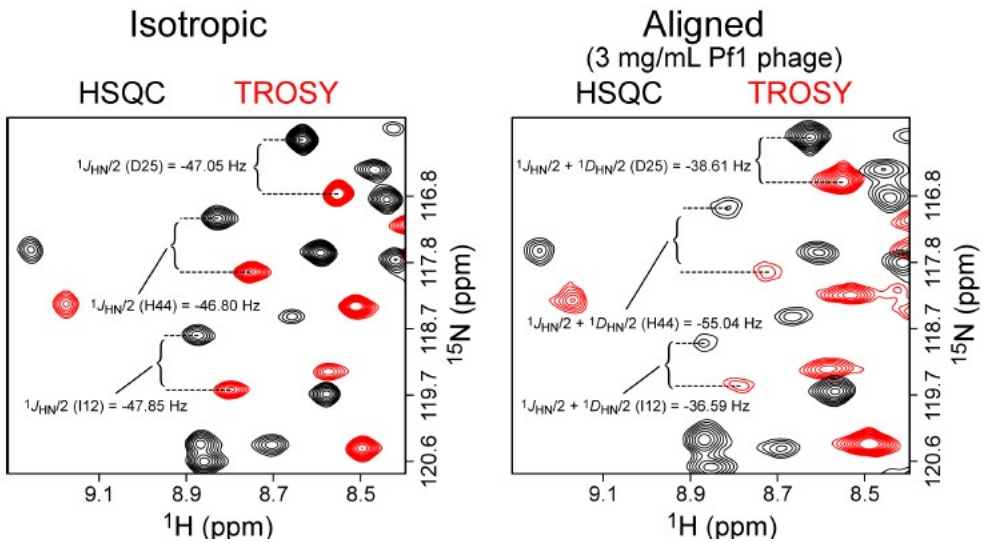

$^{1}D_{HN}$ (D25) = 16.88 Hz

$^{1}D_{HN}$ (H44) = -16.48 Hz

$^{1}D_{HN}$ (I12) = 22.52 Hz

Polyacrylamide Gels as Alignment Medium

- Liquid crystalline media can be complicated
  - concentration, temperature dependencies, some very viscous, sometimes structural changes, or tight interactions (disappearing signals), etc.
- Nice alternative is stretched polyacrylamide gels
  - at correct percentage of crosslinking (etcetera), proteins tumble isotropically in these gels (spaces in the gels large enough to accommodate isotropic tumbling)
  - when the gels are stretched, the spaces get smaller and the proteins are mechanically aligned

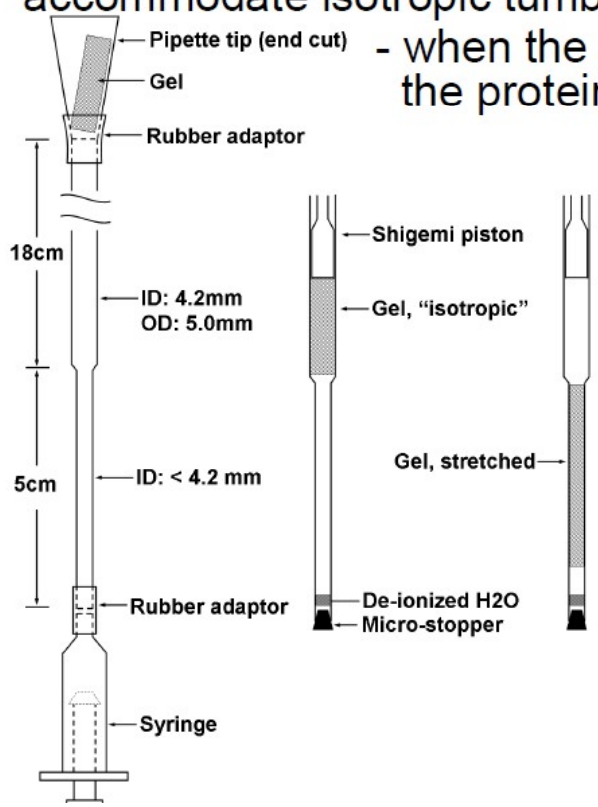

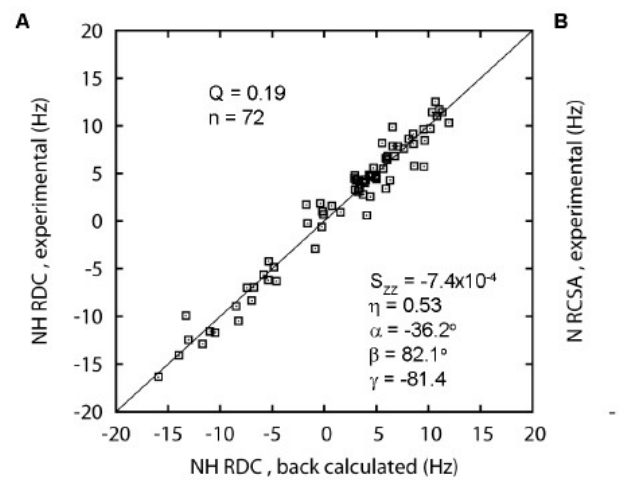

Yizhou Liu, J. Prestegard (2010)
J. Biomol NMR, **47**: 249-258.

Pulse Sequences for Collection of RDC

Table 2. Pulse Sequences Used for the Collection of Residual Dipolar Coupling Data

biomolecule	labeling	dipolar coupling	method	principle	ref
small/medium size protein	^{15}N	H_N-N	J-HSQC	J-modulation	71
			phase-encoded HSQC	peak volume in two spectra	81,196
			SCE-HSQC	line position from two spectra, normalization	98,197
			IPAP-HSQC	line position from two spectra	84,86,89
			E.COSY-HSQC	E.COSY extraction	87
			S^3E-HSQC	line position from two spectra	78
			S^3CT-HSQC	line position from two spectra	91
			α/β-HSQC	line position from two spectra	93,198
	^{13}C	$C_\alpha-H_\alpha$	CT-J-HSQC	J-modulation	82
	$^{15}N,^{13}C$		HNCO	E.COSY type spectra	199
			(HACACO)NH	J-modulation	96
			(HACACO)NH	J-modulation	96
			IPAP-(HA)CANH	line position from two spectra	107
			HCCH-COSY	line position from two spectra	90
	$^{15}N,^{13}C$	$N-C'$, $N-C_\alpha$	TROSY-HNCO	J-modulation	200
			J-correlated HNC	peak volume in two spectra	201
			SE-HSQC	line position from two spectra	202
		$C'-C_\alpha$	HN-(α/β-COCA-J)	line position from two spectra	203
	^{13}C	$C'-C_\alpha$	CT-HSQC	line position	204
		H_N-C_α, H_N-H_α	CT-J-HSQC	J-modulation	82
			S^3E-HSQC	line position from two spectra	205
	^{15}N, (10−15% ^{13}C)	H_N-C_α, H_N-H_α	soft-HNCA-E.COSY	E.COSY extraction	70
	$^{15}N,^{13}C$	$N-C'$, H_N-C'	semi-CT-HSQC	line position difference, normalization	206
			DIPSAP J-HNCO	line position in three spectra	111
			S^3E/IPAP-HNCO	E.COSY extraction	100
		H_N-N, $C_\alpha-C'$ H_N-N, $C_\alpha-H_\alpha$	IPAP-HNCO	line position from two spectra for H_N-N, from one spectrum $C_\alpha-X$	207
		$H_\alpha-N$, $C_\alpha-H_\alpha$	E.COSY HNCA	E.COSY extraction	208
		side-chain CH_2: C−H	CT-J-HSQC	J-modulation	115
			CB(CA)CONH	peak volume from three spectra	117
	$^{15}N,^{13}C$	side-chain CH_2: C−H, H−H	SPITZE-HSQC	line positions from four spectra	118
		side-chain CH_3: C−H	CT-J-HSQC	J-modulation	115

Pulse Sequences for Collection of RDC (cont.)

			CB(CA)CÖNH	peak volume from three spectra	117
	$^{15}N,^{13}C$	side-chain CH_2: C−H, H−H	SPITZE-HSQC	line positions from four spectra	118
		side-chain CH_3: C−H	CT-J-HSQC	J-modulation	115
			IPAP-CT-HSQC	line positions from two spectra	116
	$^{15}N,^{13}C$, 50% ^{2}H-fract lab	side-chain CH_3: C−H	filtered-CT-HSQC	H,H coupling as antiphase splitting	114,209
		side-chain CH_3: C−C	CT-HSQC	J-modulation	122,209
	$^{15}N,^{13}C$	side-chain CH_3: H−H	DiM	H,H coupling as antiphase split	119
	$^{15}N,^{13}C$, 50% ^{2}H-fract lab	side-chain CH_3: H−H	filtered-CT-HSQC	line separation from two spectra	120
	no label	H,H	COSY	ACME amplitude-constrained multiplet evaluation	132
			CT-COSY	intensity modulation	133,210
			signed COSY		138
			MOCCA-SIAM	ACME amplitude-constrained multiplet evaluation	211
		N−H, H_H−H_α	JHH-NOESY	E.COSY extraction	139
		H_HH_α	HNHA	J-modulation	2
	$^{15}N,^{13}C$	H_HH_α	HNCA-E.COSY	E.COSY extraction	134
	$^{15}N,^{13}C,^{2}H$	H−H	SS-HMQC	peak volume	126
			COSY-HMQC	peak volume	127
large size protein	$^{15}N,^{2}H$	H_N, N	JE-TROSY	J resolved spectroscopy in the third dimension	95
			SCE-HSQC	line position from two spectra, normalization	98
	$^{15}N,^{13}C,^{2}H$	H_N, N	TROSY-HNCO	line position from two spectra	84,102
		H_N−C_α, H_N−H_α	TROSY-HNCO	line position from two spectra	102,212
		N−C′, H_N−C′	TROSY-HNCO	line position from two spectra	102,212
	$^{15}N,^{13}C,^{2}H$	side-chain CH_3: C−C	^{13}C−^{13}C-TOCSY	H,H coupling as splitting	123
RNA/DNA	$^{15}N,^{13}C$	C−H	J-modulated HSQC	intensity-modulation	213
			TROSY-HSQC	line position from two spectra in ^{1}H dimension	214
		N9−C, $H8_N$−N9 purine N1−C, $H6_N$−N1 pyri	S^3E-HC[N]	line position from two spectra	112
			MQ-HCN	E.COSY extraction	215
		N1−C, $H1_N$-N9 purine N3−C, $H3_N$-C pyrim	S^3E-HN[C]	line position from two spectra	112
		$H_{2'}$−$H_{1'}$, $H_{2'}$−$C_{1'/2'}$, $H_{1'}$−$C_{1'/2'}$	CT-HMQC	E.COSY extraction from C1′−C2′ and H1′−C2′ planes	113
	no label	H,H	CT-COSY	intensity modulation	216
			selective-CT-COSY	peak volume	128
		H−P	CT-NOESY	intensity modulation	217
	^{19}F	H−F	E.COSY	E.COSY extraction	218,219
	$^{15}N,^{13}C$	through H bond H−N	HNN	E.COSY extraction	220
polysaccharide	no label	C−H	CT-CE-HSQC	C−H splittings	129
			HMBC	line fitting	221
		H−H	CT-COSY	intensity modulation	133
			E.COSY	E.COSY extraction	222
	^{13}C	H−H, C−C	CT-HSQC COSY	intensity modulation	223

Chemical shift anisotropy (CSA) – the complement to RDC

New techniques in structural NMR — anisotropic interactions

J.H. Prestegard

Structure determination of biomolecules by NMR has traditionally been based on nuclear Overhauser effects (NOEs). Now there are additional sources of information that can complement NOEs in cases where positioning of remote parts of molecules is important, and where extension to larger and more complex systems is desired.

of distance constraints. The approach requires not only the measurement of magnetization transfer (NOEs or nuclear Overhauser effects), but the resolution and assignment of NMR signals to specific protons, of specific residues, in a known protein sequence. Assignment of resonances and measurement of adequate numbers of NOEs have always been obstacles that made structure determination time consuming and limited to relatively small proteins (<10,000 M_r for early homonuclear studies). The limitations have been pushed back over the years with additional structural information from scalar coupling constants and chemical shifts. Assignment strategies based on the use of through bond connectivites between ^{13}C and ^{15}N sites in isotopi- to reasonably compact systems of molecular weights less than 30,000–40,000 M_r[1,2].

There have been, within the last two years, experiments reported that could dramatically change the range of applicability of NMR structural methods. Interestingly, they share an origin in anisotropic magnetic interactions that are not normally observable in high resolution NMR spectra. One important class of experiments yields structural constraints that are orientational, rather than distance based. The experiments rely on the measurement of residual dipolar couplings, and, in some cases, chemical shift anisotropy (CSA)[3–5]. The measurements can be made with great efficiency, and when combined with other recent discoveries that take advantage of more complex systems.

Residual dipolar interactions

The dipole-dipole interaction, the leading term of which is described in equation (1), is actually the basis of the NOE effect:

$$D_{ij} = -\xi_{ij} \frac{(3\cos^2\theta - 1)}{2} I_{zi}I_{zj} \qquad (1)$$

The interaction constant, ξ_{ij}, contains factors that describe the magnitudes of magnetic moments for a pair of nuclei i and j, and the internuclear distance dependence that shows up in NOE measurements. The spin operator, $I_{zi}I_{zj}$, has the same form as a first order through-bond spin-spin coupling interaction suggest-

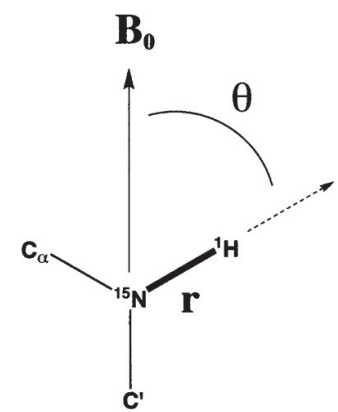

Fig. 1 Dipolar coupled ^{15}N-^{1}H spin pair in an amide bond. The bond length, r, is assumed fixed and the primary variable is the angle, θ, between the magnetic field, B_0, and the internuclear vector.

Chemical shift anisotropy (CSA) – the complement to RDC

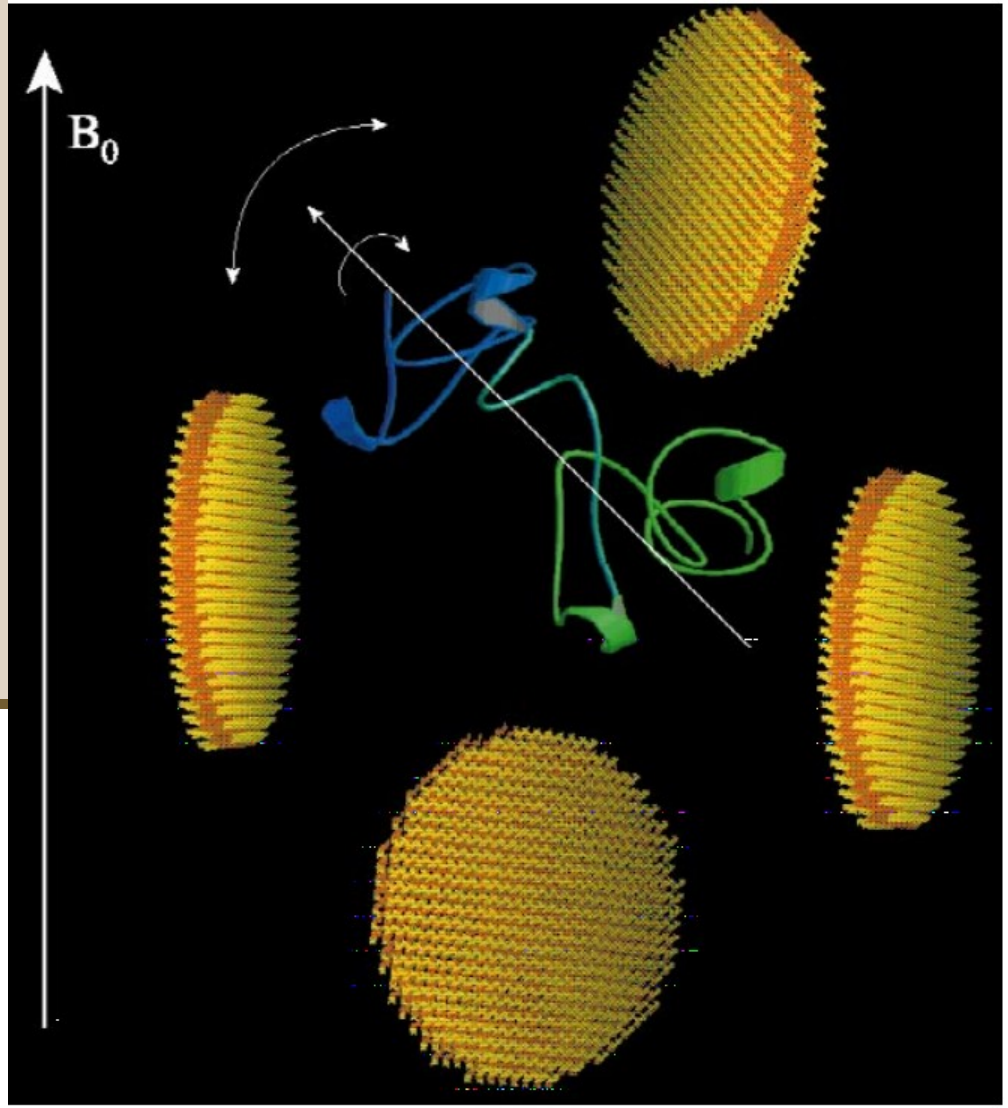

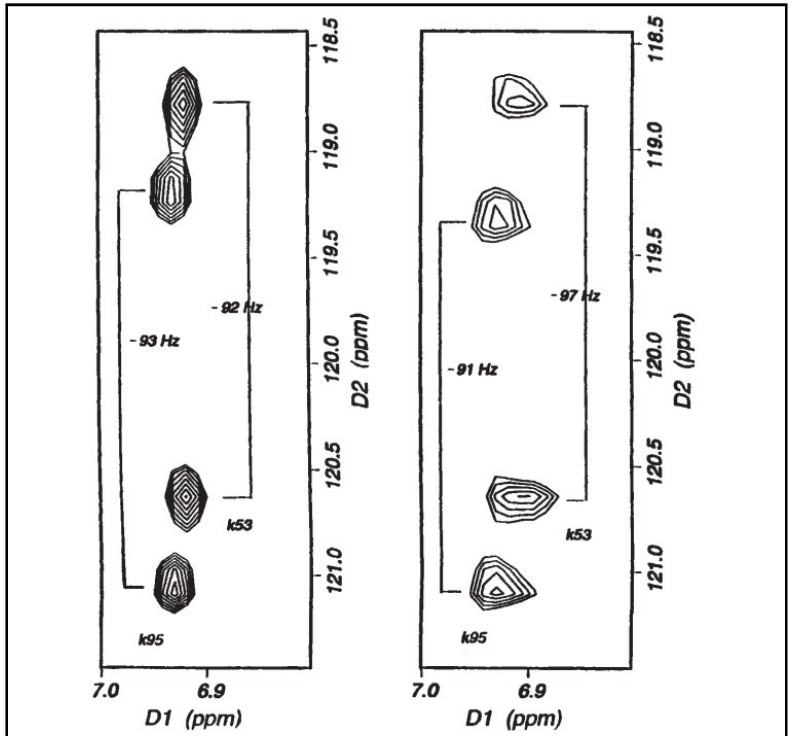

Fig. 3 Segments from a proton coupled, nitrogen decoupled, ^{15}N-^{1}H HSQC spectrum of a 0.4 mM solution of a barley lectin fragment in a 5% DMPC/DHPC 3:1 bicelle (doped with a positively charged amphiphile). Left is an isotropic spectrum at 25 °C, right is an oriented spectrum at 35 °C. Both increases and decreases in couplings are observed.

Fig. 2 Induced protein orientation by dilute phospholipid bicelles. The protein tumbles rapidly, but anisotropically, in large aqueous interbicelle spaces.

Chemical shift anisotropy (CSA) – the complement to RDC

Chemical shift anisotropy

Residual dipolar coupling is not the only anisotropic spin interaction that can provide useful structural information. Chemical shifts are also anisotropic. Nuclei which are part of various molecular functional groups resonate at different frequencies depending on shielding by the local electronic environment. Electronic environments are seldom isotropic, and hence, shielding is different for different orientations of functional groups. For the case of a molecule with an axially symmetric chemical shift tensor, the contribution to spin energy levels, which leads to an offset in resonance position from that seen with isotropic averaging, is given in equation (2):

$$C_i = \Delta\delta \frac{\overline{(3\cos^2\theta - 1)}}{2} \gamma_i B_0 I_{zi} \qquad (2)$$

The coefficient $\Delta\delta$ is the difference in chemical shift in directions parallel and perpendicular to the symmetry axis, and $\gamma_i B_0 I_{zi}$ is the Zeeman interaction operator. It is significant that an angular dependence analogous to that seen for the residual dipole interaction occurs.

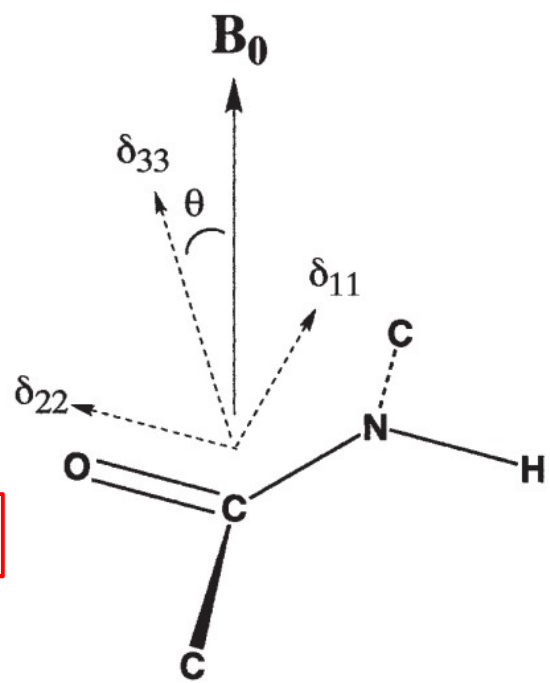

Fig. 4 Chemical shift anisotropy of an amide carbonyl carbon. Chemical shift tensor elements, δ_{11}, δ_{22}, and δ_{33}, are taken to be 223, 79 and 55 p.p.m. respectively. Shifts observed in oriented samples are functions of the angle between the magnetic field, B_0, and the principle shift tensor axes.

Solid-state NMR (powder pattern)
Chemical shift anisotropy (CSA) – the complement to RDC

- Chemical Shift Anisotropy
  - Chemical shift is dependent on orientation of nuclei in the solid
    - ***Distribution of chemical shifts***
    - ***Averaged to zero for isotropic tumbling***
    - ***Leads to extensive line-width broadening in solid-state NMR***

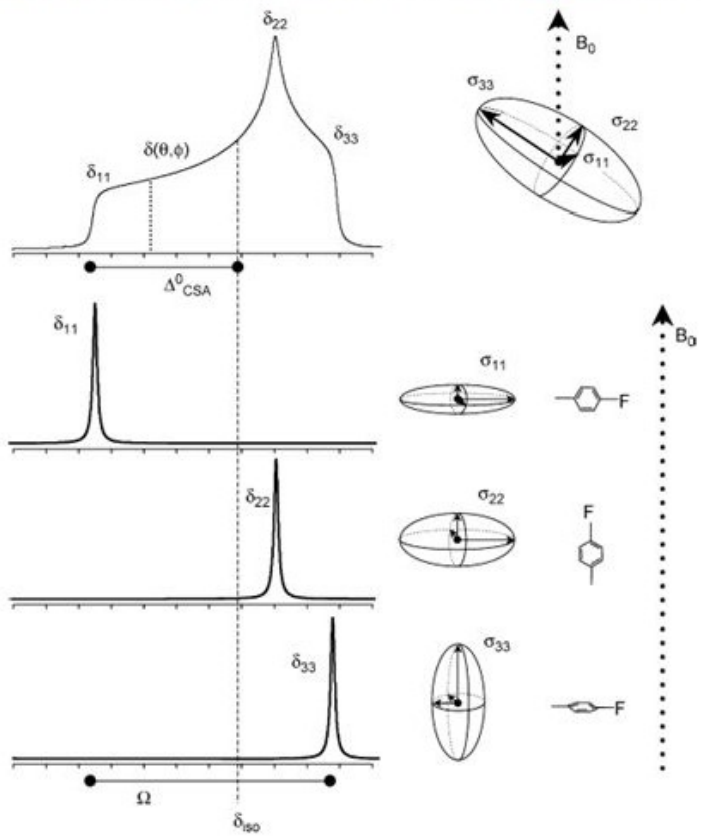

Progress in Nuclear Magnetic Resonance Spectroscopy 6 46 (2005) 1–21

Residual Dipolar Coupling (RDC) vs Switched-Angle Spinning (SAS)

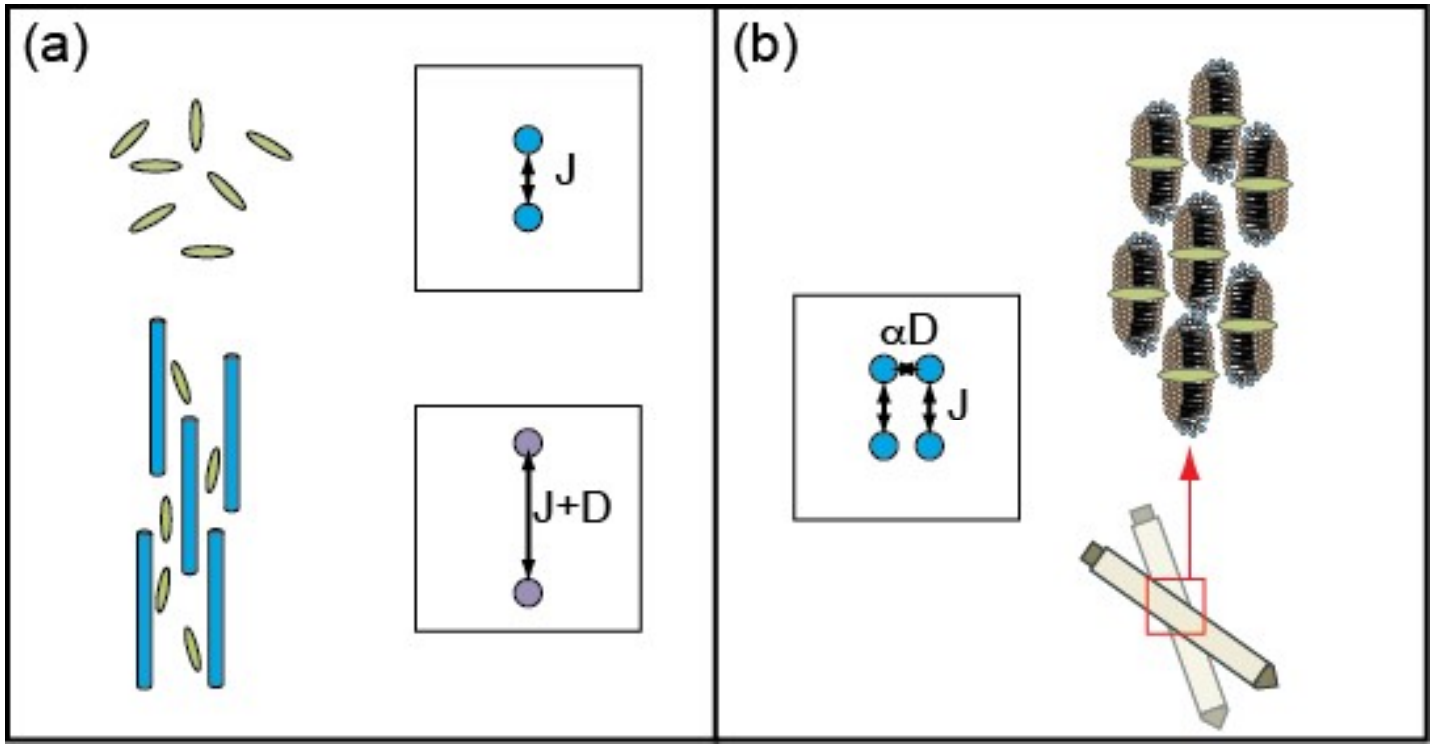

a) A solution-state residual dipolar coupling experiment, which requires separate experiments in isotropic solution and in an orienting medium. (b) An switched angle spinning (SAS) experiment, where strong orientation is produced by interaction with a membrane mimetic. The resulting dipolar couplings are scaled by changing the spinning axis without changing the sample composition or the temperature, yielding isotropic-anisotropic correlations.